Fatigue Crack Path in Non-Standard Fracture Mechanics Specimen

I. Kovše[1]

[1] Inštitut za metalne konstrukcije, Ljubljana, Slovenia. igor.kovse@imk.si

ABSTRACT. *Numerical simulation of the crack propagation in the geometrically non-standard specimen is presented. The procedure is automatic to that point that only the specimen's geometry, the starting point of the crack and material parameters are needed as input and the output of the simulation is, among other things, the crack path, the stress intensity factors and number of cycles depending on the crack length. Two-dimensional finite element method is used in the calculations. Crack growth is simulated in a series of crack increments of finite size. Finite element mesh is automatically generated after each crack increment. Numerical results are compared to the results of the experiment on a specimen with non-standard geometry. During the experiment the crack length was measured automatically from the compliance of the specimen. Experimentally determined fatigue crack evolution is approximated by a 4-parameter empirical function, the derivative of which is used to describe the crack rate vs. stress intensity factor relationship.*

INTRODUCTION

The influence of the cracks on a structure can be indirectly considered through their influence on material parameters. This "smeared crack" approach is usually used in damage mechanics. The direct approach used in fracture mechanics is to consider actual configuration of the crack(s) as two distinct but geometrically coincident surfaces. This second approach is used throughout the present paper.

Basic analysis of cracks in the structure can be presented in form of two following relationships:

$$K_I(a,P) \le K_{Ic} \tag{1}$$

$$\frac{da}{dN} = F(K_I(a,P)) \tag{2}$$

The first inequality is the relation between the bearing capacity of the structure or part of it and the size of the crack. K_{Ic} is fracture toughness and is considered as material parameter and the stress intensity factor K_I is numerical value depending on the geometry of the structural element containing the crack, the load P and the crack length a. The equality in Eq. 1 means that a critical state is reached, possibly leading to structural failure.

Equation 2 represents the time evolution of the crack in term of crack growth rate *da/dt*. The function *F* is determined from the dynamical experiment in which the specimen is exposed to a load *P* that is periodically changing in time *t*.

The analysis is thus a combination of numerical and experimental methods, where we use numerical calculations to determine the relation $K_I(a,P)$, and experiments to establish material parameter K_{Ic} and the function *F*. In this paper the procedure is shown for a non-standard fracture mechanical specimen called CTN, which is slightly changed standard CT specimen. We could consider it as a detail that it critical for the behaviour of hypothetical structure. With the non-standard geometry we wish to show how principles of fracture mechanics, with suitably developed numerical and experimental methods, can be successfully applied in the analysis of fatigue crack propagation of an arbitrary structural detail.

NUMERICAL SIMULATION

Numerical simulation of fatigue crack growth, which is presented in this paper, is based on the two-dimensional finite element method (FEM).

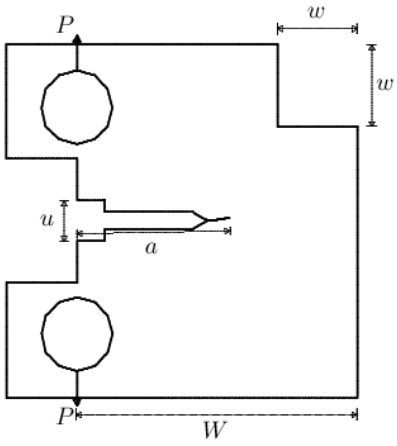

Figure 1. The contour of the CTN specimen as the input to the numerical analysis.

Input data for the simulation are the contour of the plane region describing the model geometry, the point where the crack propagation starts and the material characteristics of the model. In our case it is the contour of the CTN specimen from Fig. 1 with the dimensions: width W=50 mm, thickness B=25 mm, starting crack length a_0=24.5 mm and the dimension of the cutout w=14 mm. Similar specimen shape has been used by Lining [1]. Linear elastic material model was chosen with usual parameters for steel: Young modulus E=2.1 10^5 MPa and Poisson's ratio ν=0.3. Plane strain was assumed.

Crack growth was simulated with a series of discrete crack increments Δa. Automatic generation of finite element mesh over the whole domain was used after each crack increment (Fig. 2). The mesh generator is based on the algorithm of Zhu et.al. [2] and is described in more detail by Kovše [3]. After each mesh generation the displacement, deformation and stress fields were calculated according to standard FEM procedure and then the following parameters of LEFM (linear elastic fracture mechanics) were calculated: stress intensity factors K_I, K_{II}, J-integral, strain energy release rate G and the direction of crack growth ϕ. The crack was then extended by a suitable increment length in the direction ϕ and the procedure was repeated.

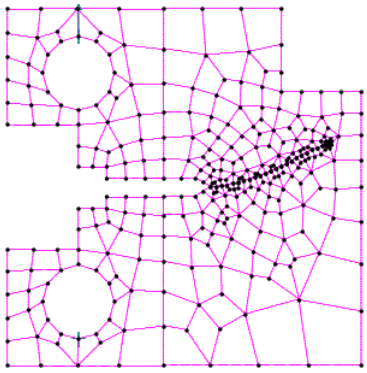

Figure 2. The finite element mesh generated automatically at the crack length a=39 mm.

The fracture mechanics' parameters were calculated using the virtual crack extension (VCE) method. The method consist of extending the crack tip for a small distance (of the order 10^{-4} of the length of the finite element at the crack tip), and calculating the strain energy release rate G from the difference of potential energies before and after the crack tip extension. It can be shown (see Hellen [4]) that with this method only one finite element calculation is needed for the determination of G. With the separation of displacement field on the symmetrical and non-symmetrical part (e.g. Xie et.al. [5]) we can calculate G_I and G_{II} , which correspond to the first and second fracture mode respectively, and accordingly K_I and K_{II} . The angle ϕ represents the direction of the next crack increment. We can determine ϕ using different methods: (a) from the analytical expression $f(K_I(\phi),K_{II}(\phi))=0$ corresponding to the maximal tension stress direction (see e.g. Evald and Wanhill [6]); (b) as a direction of maximal strain energy release rate G; (c) as a direction perpendicular to the internal force $\boldsymbol{F}$ at the crack tip. The internal force $\boldsymbol{F}$ is associated with the finite element mesh at the crack tip and is calculated as a reaction by which elements on the upper face of the crack act upon the elements on the lower face of the crack [7]. Most of the results in this paper are based on the second method, numerical implementation of which was extending the crack tip in different directions and finding the direction where G was maximal.

Using the above procedure with a series of successive crack increments a geometry of the crack path is obtained as well as the dependence of fracture mechanics parameters on the crack length a: $K_I(a)$, $K_{II}(a)$, $J(a)$, $G(a)$, $\phi(a)$. The compliance dependence on crack length $c=a(a)$ is also obtained. It is used for crack length measurement during the experiment.

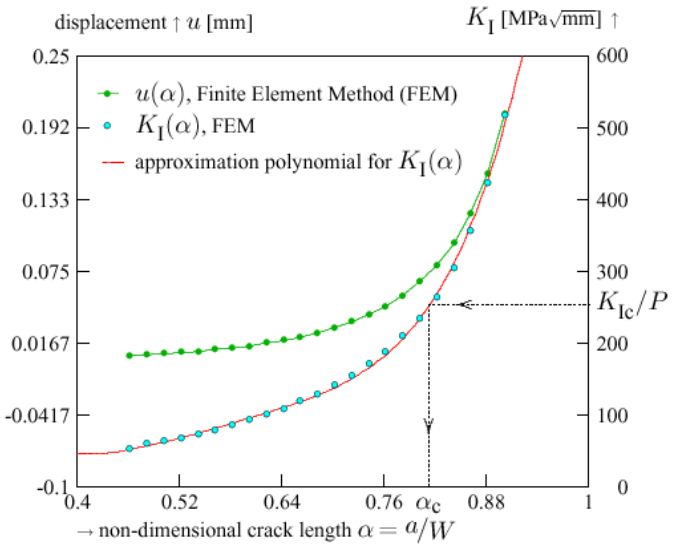

Figure 3. FEM analysis. The dependencies $u=u(\alpha)$ and $K_I=K_I(\alpha)$ for the CTN model and the unit force P=1 kN.

The relationship $K_I=K_I(\alpha)$ for the CTN model is presented on Fig. 3. With $\alpha=a/W$ we denoted the non-dimensional crack length. If we know the fracture toughness of the material K_{Ic}, we can determine the critical crack length $a_c=\alpha_c W$, as indicated in Fig. 3. The crack does not propagate in a straight line in the CTN specimen (see Fig. 5). In this paper we define the crack length a as the arc length - although other definitions of the crack length could also have been taken.

Second Order Crack Path Simulation

The crack path can be represented as a parametrically defined curve $\boldsymbol{r}$ in two dimensional space, using the crack arc length a as the natural parameter. The vector $\boldsymbol{r}$ and its derivative are:

$$\boldsymbol{r}(a) = (x(a), y(a)), \qquad \boldsymbol{t} = \boldsymbol{r}' = (\cos(\phi(a)), \sin(\phi(a))) \tag{3}$$

Simulating the crack growth with successive discrete crack increments, as presented above, is actually the first order (Euler) integration of Eq. 3. The method requires only one calculation of the tangent vector $\boldsymbol{t}$ at each step, but the calculated path diverges quickly from the exact one, unless very small crack length increments Δa_i are used.

A better method is the one of the predictor-corrector type. This method requires two calculation of the tangent vector $\boldsymbol{t}$ at each step. In this section we show the predictor-corrector method for variable crack arc length increments $\Delta a_i=a_i-a_{i-1}$ with the mid-point integration rule for predictor and trapezoidal integration formula for corrector. We will consider only the coordinate x, the development for the coordinate y being identical. The formulas for the predictor $x^{(p)}$ and the corrector $x^{(c)}$ at crack increment $i+1$ are:

$$x^{(p)}{}_{i+1} = x_{i-1} + (1+\gamma)\Delta a_i \cos\phi_i \qquad x^{(c)}{}_{i+1} = x_i + \gamma\Delta a_i \frac{1}{2}(\cos\phi_{i+1} + \cos\phi_i) \qquad (4)$$

With the assumption that the third derivative x''' is constant, we can estimate the local error of the corrector $\varepsilon^{(c)}{}_{i+1}$ (see detailed development in [7]):

$$\varepsilon_{i+1}^{(c)} = -\Delta x_{i+1} \frac{(1+\gamma)^3}{\frac{(1+\gamma)^3}{2} + \gamma^3} \qquad (5)$$

When the maximal permissible error ε is given, and the interval Δa_i is known, we can calculate the length of the interval $\Delta a_{i+1}=\gamma\Delta a_i$. at which the error in crack coordinate will be less or equal to ε.

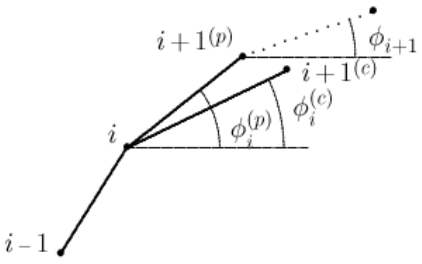

Figure 4. The determination of the crack path with the predictor-corrector method.

The determination of the crack path increment with the predictor-corrector method is shown on Fig. 3. In the increment i we first calculate the angle ϕ_i and determine the predictor coordinates with Eq. 4. After extending the crack, the new FEM model is constructed and solved and the crack growth angle ϕ_{i+1} is calculated. If the error $\varepsilon^{(c)}{}_{i+1}$ in increment i is bigger than the permissible one, the procedure is repeated for step i with smaller crack increment, otherwise new crack increment length is obtained and the procedure repeated for the next step $i+1$.

FATIGUE EXPERIMENTS AND COMPARISON WITH THE CALCULATION

In order to determine the law F from Eq. 2 we make the experiment in which the specimen is loaded with periodically changing force with frequency f and amplitude $\Delta P=P_{max}-P_{min}$ for a certain period of time or accordingly with a certain number of load cycles. During the experiment the number of cycles N is counted and crack length a is measured from the compliance $c=c(a)$.

In the following we present the results of the experiment and the calculation for the CTN specimen. We conducted the experiment with the CTN specimen loaded with cyclic loading frequency f=4 Hz, constant amplitude ΔP=10 kN and with the ratio $R=P_{min}/P_{max}$=0.2. In Fig. 5 we give the comparison of the crack path at the end of the experiment and the crack path obtained by numerical simulation.

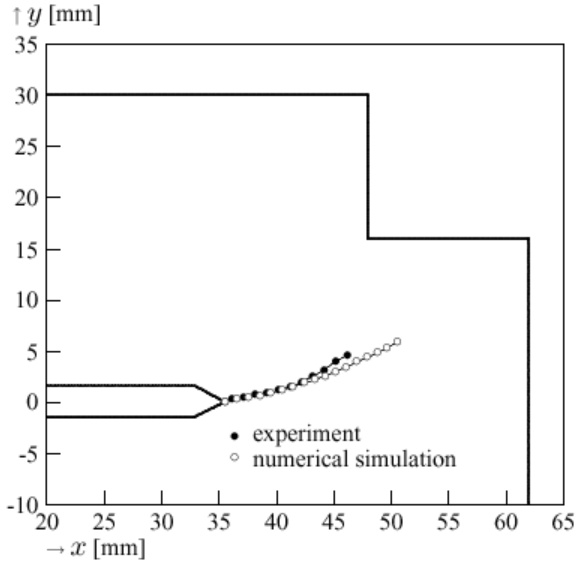

Figure 5. Comparison of numerically simulated crack path with the experimental one.

During the experiment the crack length a was continuously determined from the compliance. To assess the accuracy of this method we measured the crack length at several time intervals also using the optical microscope. The comparison of both methods is shown in Fig. 6.

To determine the function F from Eq. 2 we need to calculate the derivative da/dt or da/dN. Direct calculation of the derivative da/dN from the measured pairs of values (a,N) (i.e. numerical differentiation) is not recommended, because it produces large scatter due to measurement and numerical inaccuracies (see Smith and Hooeppner [8] and Fig. 7). We rather approximated the measured relationship $a=a(N)$ with exponential function $y(N)=A+e^{(C\ N+D)B}$ (shown in Fig. 6). The crack growth rate is then the derivative of this function: $da/dN=dy/dN=y'$. The unknown coefficients A, B, C, D were fitted using the special procedure (Smith and Hooeppner [8]):

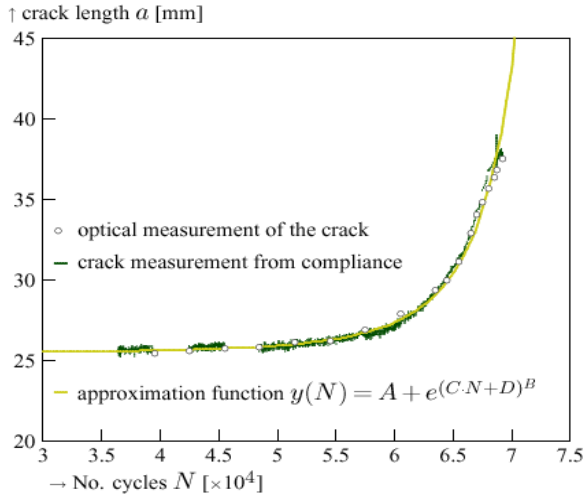

Figure 6. Crack length as a function of the number of cycles. Comparison of two measurement methods: optical and compliance methods.

A=24.5, B=9.9902, C=11.02 10^6, D=0.3417

With the known functions $a=y(N)$, $da/dN=y'(N)$ and $K_I(a,P)=K_I(y(N),P)$ we know also the relationship F. For the CTN specimen this relationship is shown in Fig. 7. We can use it for the integration of Eq. 2 instead of the standard Paris law, which represents the linearisation of the portion of this relationship in the logarithmic scale.

CONCLUSION

Numerical and experimental analysis of the fatigue crack propagation in the geometrically non-standard specimen was shown. The numerical simulation is made considerably easier with the use of the automatic generation of the finite element mesh after each crack increment. With this simulation we can obtain the dependence of the arbitrary fracture mechanical parameter on the crack length. The crack path of non-symmetrical i.e. curved cracks can be predicted with sufficient accuracy. The results of the simulation can also be used to measure crack length in arbitrary shaped specimen continuously during the fatigue experiment. It has been shown that with the use of approximation functions the crack growth rate law can be more suitably modelled than with the Paris line, which represents just a portion of that law. This can be important for the more realistic prediction of the remaining life of a structural component.

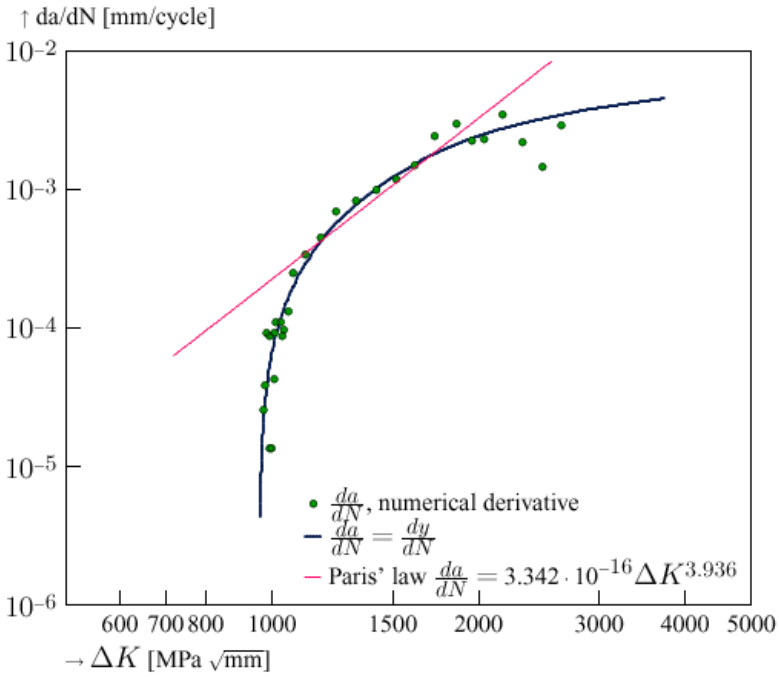

Figure 7. The crack growth rate law from the experiment on the CTN specimen. The values of *da/dN* are obtained with numerical differentiation of the measured values and with the differentiation of the approximating function *y(N)*. Also shown is the Paris line.

ACKNOWLEDGEMENT

The author wishes to thank the Ministry of education, science and sport of Slovenia for the financial support of the project.

REFERENCES

1. Lining, W. (1993) In: *Mixed-Mode Fatigue and Fracture, ESIS 14*, pp. 01-215, Rossmanith, P. (Ed.), Mechanical Engineering Publications, London.
2. Zhu, J.Z., Zienkiewicz, O.C., Hinton, E., Wu, J. (1991) *Int. J. Num. Meth. Engng* **32**, 849-866.
3. Kovše, I. (1996) In: *Localized Damage IV: Computer-Aided Assessment and Control*, pp. 935-942, Nisitani, H. (Ed.), Computational Mechanics Publications, Southampton.
4. Hellen, T.K. (1975) *Int. J. Num. Meth. Engng* **9**, 187-207.
5. Xie, M., Gerstle, W.H., Rahulkumar, P. (1995) *J. Engng Mech. (ASCE)* **121**, 914-923.
6. Evalds, H.L., Wanhill, R.J.H. (1985) *Fracture mechanics*, Edward Arnold in Delftse Uitgevers Maatschappij, Delft.
7. Kovše, I. (1998) PhD Thesis, University of Ljubljana, Slovenia.
8. Smith, F., Hooeppner, D.W. (1990) *Engng Fract. Mech.* **36**, 173-178.